Nuclear Instruments and Methods 201 (1982) 309–313
North-Holland Publishing Company

A POLARIMETER FOR PROTONS BETWEEN 100 AND 800 MeV

R.D. RANSOME*, S.J. GREENE** and C.L. HOLLAS
University of Texas at Austin, TX 78712, U.S.A.

B.E. BONNER, M.W. McNAUGHTON, C.L. MORRIS and H.A. THIESSEN
Los Alamos National Laboratory, Los Alamos, NM 87545, U.S.A.

Received 11 February 1982

A carbon polarimeter has been built and used for protons with energies between 100 and 800 MeV. The polarimeter accepts scatters in the carbon analyzer up to 30°_{lab}, with negligible instrumental asymmetries. Drift chambers 60 cm square were used with a system for resolving the left–right ambiguity inherent in drift chambers. A hardware system for rejecting small angle scatters is described. The polarimeter is routinely used to measure spin transfer parameters with a typical precision of ± 0.03 in about eight hours of low-duty LAMPF beam.

1. Introduction

In the past few years a number of medium energy measurements of p–p and n–p Wolfenstein parameters have been reported. These experiments require a device to measure the polarization of scattered or recoil protons. Two such polarimeters have been used at TRIUMF [1] and SIN [2], and two are in use at LAMPF, namely the HRS focal-plane polarimeter [3], and the device known as JANUS, reported here.

This polarimeter has a slightly larger acceptance angle from the carbon analyzer than the other polarimeters. It also uses multiple wire drift chambers (MWDC) rather than multiple. wire proportional chambers (MWPC), giving finer spatial resolution with very low instrumental asymmetries. Following are descriptions of the polarimeter, the electronic logic, and characteristics of the polarimeter (efficiency and instrumental asymmetries).

2. Polarimeter

Fig. 1 shows a schematic of the polarimeter. It consists of two identical scintillator assemblies (SF and SB), six identical drift chambers, and a variable thickness carbon analyzer. Protons with polarization P_y scatter from the carbon with an azimuthal distribution of the form

$$N = N_0\left[1 + P_y A_c(\theta)\cos\phi\right], \tag{1}$$

where $A_c(\theta)$ is the carbon analyzing power, known from the global fit described in our accompanying paper [4]. (Horizontal components P_x would add a $\sin\phi$ term, while small higher order terms may appear as a result of undesirable instrumental asymmetries.) The polarization P is then obtained by Fourier analysis, as described in refs. 4–6.

SF and SB each consist of two 0.476 cm × 30.5 cm × 61.0 cm pieces, individually wrapped. The two pieces overlap slightly. Each scintillator is viewed by an EMI9813 photomultiplier at each end.

The drift chambers are similar to those described in ref. 7. Each drift chamber has a nominal active area of 60 cm × 60 cm, and consists of two signal planes, with

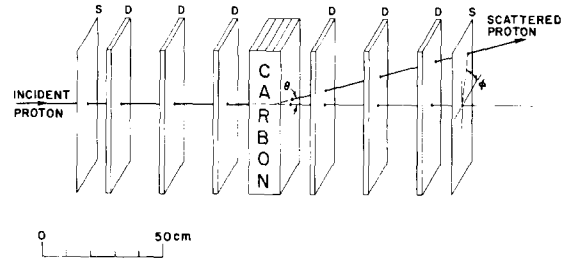

Fig. 1. Scale drawing of the polarimeter. S represents a scintillator, D represents a multiwire drift chamber (XY pair). The incident proton scatters in the carbon through polar and azimuthal angles θ, ϕ. The polarization of the incident proton is obtained from the azimuthal distribution of events [eq. (1)].

* Present address: Max Plank Inst. für Kernphysik, Heidelberg, West Germany.
** Present address: New Mexico State University.

0167-5087/82/0000–0000/$02.75

wires perpendicular to each other, three cathode planes, and two cover planes. The sequence is cover, cathode, "x" signal, cathode, "y" signal, cathode and cover plane spaced 4.8 mm apart. Cathode planes are 13 μm Al foil. Signal planes, fig. 2, consist of alternating anode and cathode (field shaping) wires. Wires are evenly spaced with a 0.4064 cm separation. Anode wires are 20 μm gold-plated tungsten, cathode wires are 76 μm gold plated copper clad aluminum. A positive 2250 V is applied to the anode wires, while the cathode wires and planes are at ground. A standard "magic" gas mixture of 62% argon, 38% iso-butane, 0.1% isopropyl alcohol, and 0.03% Freon is used.

Each anode wire is attached to a 200 ns long delay line, with a nominal 2.8 ns per wire separation. Signals from the delay line ends are fed to discriminators located near the polarimeter. A discrimination level of about 2.7 mV is used to obtain precise signal timing.

Although drift chambers are capable of good spatial resolution, an ambiguity exists in determining on which side of the signal wire each event occurred. As reported by Atencio [7], Walenta [8] and Breskin [9], this ambiguity can be resolved by examining the induced pulses on the cathode wires. The induced pulse on the cathode wire nearest the event has an amplitude about 10% larger than the induced pulse on the cathode wire on the opposite side of the anode. By subtracting the two pulses, the side of the anode on which an event occurred can be determined. The comparison of pulse heights is made by attaching alternating cathode wires to two bus

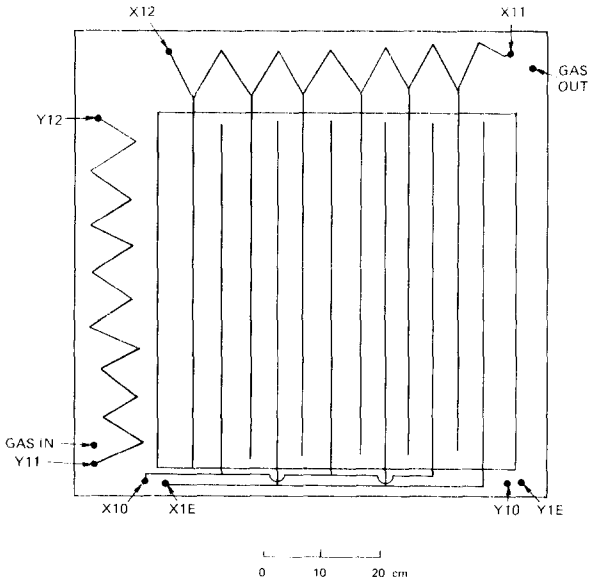

Fig. 2. Schematic of a drift chamber signal plane. The sawtooth line represents a delay line. Alternate drift wires are read out as odd (X1O, etc.) or even (X1E, etc.). The wire spacing is not to scale.

Table 1
Fraction of events scattering usefully ($\phi_c \geq 2.9°$) as a function of proton energy incident on the carbon, and carbon thickness.

Energy (MeV)	Thickness (cm)	Fraction
650–800	25.4	0.080–0.100
400–650	12.7	0.039–0.046
200–400	6.4	0.010–0.017
100–200	3.2	0.005–0.010

lines (fig. 2), referred to as "odd" and "even" lines for convenience. These two lines are then fed into an electronic unit [10] which adds (O + E output) and subtracts (O – E output) the pulses. The subtracted pulse is integrated over the first 100 ns of the pulse with a charge sensitive analog-to-digital converter (ADC) and the output used to determine whether the event occurred on the "odd" or "even" side of the anode wire. More details of this system follow below. The O + E output has a long pulse length (around 1 μs), which introduces an undesirably long dead time into the system. This was reduced by clipping the output with a 3.65 m long line, reducing the pulse width to an acceptable 200 ns.

The carbon analyzer consists of commercial grade ATJ graphite, with a measured density of 1.75 g/cm^3. The thickness is variable from 3.2 cm to 25.4 cm in 3.2 cm steps, by bolting thin 60 cm square plates together. This thickness range allows the polarimeter to be efficiently used for proton energies between 100 and 800 MeV (see table 1).

The drift chambers, the carbon, and scintillators are all mounted in movable rectangular frames. Each corner of the frame rests on a linear translation bearing which slides over a rail, with the rail being mounted to a rigid outer steel frame. The maximum front to back spacing of the scintillators is about 150 cm. The entire assembly weighs about 1500 kg, and sits on a three-wheeled table, allowing it to be moved. Each wheel can be lowered or raised to provide the desired height and level for the polarimeter. The outer frame is rigid enough to allow the entire instrument to be lifted by crane.

3. Logic and hardware reject of small angle scatters

The logic for each of the 12 wire planes is identical. The master trigger (an "event") is a coincidence of SF and SB, and is used to start three time to digital converters (TDC). Discriminated signals from the delay line ends are used to stop two of the TDCs, while the third stop is provided by the O + E signal. The master

trigger also provides a gate for integration of the O − E signal. All TDCs and ADCs are commercially available CAMAC units and are interfaced to a PDP-11 computer. Each event is written to magnetic tape for off-line analysis.

The anode wire which fired (n) and drift time (d) can be determined from the following relations:

$$T_1 = S_1 + d + nD,$$

$$T_2 = S_2 + d + (N - n)D,$$

$$T_{oe} = S_3 + d,$$

T_1 and T_2 are the times from the delay line ends, T_{oe} is the time from the O + E output, D is the delay per wire, N the number of wires (73), and the S's are constant offsets relative to the master trigger. The difference in the times from the delay line ends ($T_1 - T_2$) is proportional to the wire number n (plus a constant) and the O + E time is equal to the drift time plus a constant. Since all three times involve the drift time, a consistency check can be made by using the relation

$$\text{CKSM} = T_1 + T_2 - 2T_{oe} = ND + S_1 + S_2 - 2S_3. \qquad (2)$$

The checksum (CKSM) involves only constant values, so it should be a constant for good events. Events in which the checksum falls outside of narrow limits can be software rejected.

Since small angle (less than 3°_{lab}) scatters have a small analyzing power and the largest uncertainty in the azimuthal scattering angle, it is desirable to eliminate them from the data stream, both to allow a higher rate of good events, and to reduce the amount of magnetic tape needed for an experiment. A fast analog system for rejection of small angle scatters was developed for this polarimeter, the circuit for which is shown in fig. 3. The first, third, fourth, and sixth drift chambers are used. An estimate of the wire position is made for each plane by starting a time to amplitude converter (TAC) with the signal from one end of a delay line and stopping the TAC with the signal from the other end. Differences in slopes in the x–z and y–z (horizontal and vertical planes) are estimated from the sums (X6 − X4) − (X3 − X1) and (Y6 − Y4) − (Y3 − Y1) using analog summing amplifiers. The sums are then fed into a single channel analyzer (SCA) and a window set to allow only sums corresponding to changes in slope of zero or one wire to give an output. If both x and y planes have small slopes, the event is rejected. The decision process takes about 8 μs. No attempt is made to use the drift time information, so the spatial resolution for each plane is ± 0.4064 cm, corresponding to 1.0° for the present spacing of 22.2 cm between planes. The desired rejection area is the circle formed by scatters of three degrees or less. Since the system can reject only the square area formed by slope changes of zero or one wire the maximum efficiency is 64% ($2r^2/\pi r^2$). The system does reject about 60% of the scatters less than 2°, but only 20% of those scattering between 2° and 3°. No events with scatters greater than 4° are rejected. The system also rejects those events in which one or more ends of the delay lines did not fire. This system increases the ratio of good events to total events written to tape by a factor of two to three, depending on the carbon thickness being used.

Another hardware reject system was developed to reject those events in which the three positions measured by each set of three planes before and after the analyzer do not lie on a straight line. Such events result

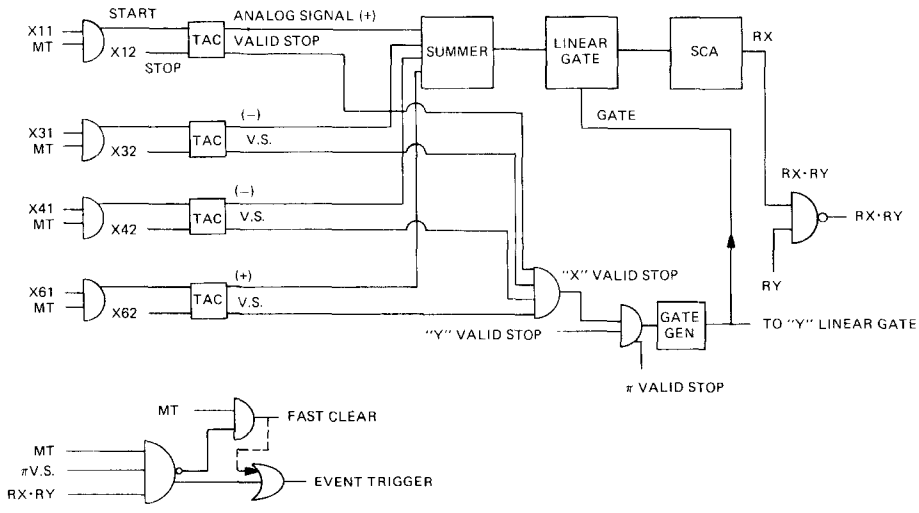

Fig. 3. Fast clear and event trigger logic. XIJ = track timing pulse from delay line of chamber J. MT = master trigger from scintillator. πVS = product of valid TAC stop signals on all chambers.

predominantly from the production of δ rays, as mentioned in section 4. The circuit for this is essentially the same as that used for the small angle scatter reject system. The difference is that the sums formed are (X3 + X1 − 2X2), (X6 + X4 − 2X5), and the similar sums for the "y" planes. The two reject systems used together increase the ratio of good events to total events on tape by about a factor of 5.

4. Characteristics of the polarimeter

The most important aspects of the polarimeter are: spatial resolution, solid angle, efficiency, and instrumental asymmetries. Each of these will be discussed below, as well some aspects of the odd–even system.

The use of three chambers before and after the analyzer makes a check of the spatial resolution possible. The position in the center chamber can be calculated from the positions in the outer chambers. The difference between measured and calculated positions in the center chamber (the residual) is a measure of the resolution. We observe a peak with a r.m.s. width of about 0.15 mm, indicating a chamber position resolution on the order of 0.1 mm. This high resolution allows a closer spacing of the drift chambers (hence larger solid angle) than would be possible with individual wire readout systems to achieve the same angular resolution.

Proton carbon scattering with angles up to about 30° can be measured. Acceptance greater than this is not needed, since the cross section is small and in the energy range measured the analyzing power is also small at larger angles.

Chamber efficiency can be defined several ways. If one simply checks when a plane does not record an event and adjacent planes do, the plane efficiency is quite high, $>99.5\%$. A more pertinent measure is the fraction of events which have a good "checksum" [eq. (2)] for each plane. For singles rates in the chambers below about 10^4 Hz, this is also reasonably good, $\sim 99\%$. An efficiency for the entire system can be defined by the percentage of total events which have a good checksum in all 12 planes, and good residual for all four sets (front and back x and y). This is typically 60–70%. This low efficiency is due primarily to delta rays (high energy electrons), which are produced mainly in the front scintillator and the analyzer. Delta rays decrease the efficiency of the system in the following manner. The maximum drift time is rather long (about 80 ns). Thus, if a proton gives a long drift time, but produces an electron with a short drift time, the electron's position will be recorded instead of the proton's. This event will have a good checksum, just like a good proton event. Since all but the highest energy deltas will have a range less than one chamber spacing, all other planes will record the proton's position, leading to a bad residual for one set of planes. Sauli [11] has calculated the number of delta rays produced in a gram of material. The level of bad residuals observed in our system is consistent with his calculations.

One final measure of the efficiency is the number of events scattering greater than 3°, along with good checksums and residuals. This varies with energy and the carbon thickness (see table 1). For 800 MeV protons with 25.4 cm carbon and without the small angle reject system in use, this is about 8%. With the small angle reject and the hardware residual system in use, this efficiency increases to about 40%.

Instrumental asymmetries [4,5] have been examined in a variety of ways, e.g., by comparing results with the beam spin reversed, scattering to both left and right of the beam, and using Fourier analysis to extract the coefficients of $\cos(n\phi)$ and $\sin(n\phi)$ for $n = 1,5$ (e.g., see appendix E of ref. 5). In all cases, the result has been consistent with an overall effect $\leqslant 0.005$. In most cases use of the $\phi + \pi$ test [4,6] and reversal of the beam cancel this effect at least to first order. The only significant exception is in the extraction of carbon analyzing power from the scattered beam [4] in which at worst the instrumental asymmetry gives an error comparable to the statistical uncertainty.

There are two known causes of the instrumental asymmetries. In the very earliest data [13,14], the fast clear was not properly adjusted to take account of the different delay line speeds of different chambers. This asymmetry affected only the smallest angle bins ($<5°$). A second problem affected only events at the edge of the back chamber. At the extreme edge, and for long drift times, the total time (delay line plus drift time) exceeded the TDC range, so TDC time-out reduced the chamber efficiency.

The odd–even system described earlier was found to give good results. The ADC spectrum consists of two well separated peaks, with about 94% of the events in the peaks. The median of the spectrum was used as a dividing point to decide on which side of the signal wire the event occurred. The effectiveness of the system was determined by examining the residual spectra. The spectra show a sharp peak (fwhm ~ 0.3 mm) with a small plateau at the base. By switching the event position from one side of the wire to the other side for one plane at a time, and recalculating the residual, a check for a failure of the ADC system can be made. Only one plane at a time out of each set of three (X1–X2–X3, X4–X5–X6, etc.) is allowed to have a position opposite the original. If the combination which gives the smallest residual is used, the plateau is nearly eliminated. This indicates the odd–even system fails for about 1% of the events per plane. During final analysis, we have done this odd–even check for each set and used as the final positions in the planes the combination which gives the smallest residual. No instrumental asymmetries were introduced by this procedure.

5. Software checks and corrections

A number of calculations and corrections must be made in the software to determine the final position of each event. The most important of these are the calculation of the correct anode wire from the delay line TDC information and the determination of the distance of the event from the anode wire (drift position) from the O + E TDC.

Although the difference of the two times from the delay line ends A is nearly linear with the wire number, small non-linearities in the TDCs and delay line make a correction necessary. This is accomplished by expanding to third order

$$AP = R_1 + R_2 A + R_3 A^2 + R_4 A^3.$$

The constants $R_1 - R_4$ are chosen such that AP is in centimeters.

The drift position is determined from the O + E time which is equal to the drift time plus a constant. By assuming the events are evenly distributed over one wire spacing, a look-up table is formed to relate drift position to O + E time. Corrections are made for the propagation time of the pulses as a function of (crude) position, and to correct for differences in the TDC calibration constants, so the same look-up table can be used for each plane.

The final position in each chamber is given by XY = TAP + Sign * DPOS + C where TAP is the anode position truncated to the nearest wire, DPOS is the drift position, and SIGN is derived form the O − E ADC (section 2). The software alignment constant C is determined to ±0.1 mm by examining straight tracks of high energy protons with the carbon removed.

A few other checks are made on the final results. A final good event includes a cut on the checksum peak for all 12 planes and a cut of ±1.0 mm on the residual for each of the four sets of planes. A requirement is also made that the distance of closest approach between the ray calculated from the front chambers and the ray calculated from the back chambers be within 5 mm, and that the position of closest approach be within the carbon. No requirement is made on the time-of-flight between the front and back scintillators. Consequently the events from the carbon are inclusive, subject only to the weak requirements that there be a single charged particle track in the back scintillators, and that the particle have enough energy to reach the back scintillator without excessive (~ 100 mr) multiple scattering through the three chambers and without excessive (~ 10 ns) delay.

Further details of this polarimeter are contained in two reports [5,15], which may be obtained from the authors.

6. Conclusions

We have built and successfully used [13,14] a large solid angle polarimeter over a wide range of energies. The polarimeter has high resolution with low instrumental asymmetries. A hardware reject system gives the system an efficiency of about 40%.

We wish to thank the BASQUE group [1] for sharing their experiences with us. We also thank L. Atencio for his excellent work with the drift chambers.

This work was supported in part by the U.S. Department of Energy.

References

[1] G. Waters et al., Nucl. Instr. and Meth. 153 (1978) 401.
[2] D. Besset et al., Nucl. Instr. and Meth. 166 (1979) 379.
[3] J. McClelland et al., to be submitted to Nucl. Instr. and Meth.
[4] R.D. Ransome et al., Nucl. Instr. and Meth., this issue, p. 315.
[5] R.D. Ransome, Dissertation, Univ. of Texas at Austin (1981) and Los Alamos Report LA-8919-T (unpublished).
[6] D. Besset et al., Nucl. Instr. and Meth. 166 (1978) 515.
[7] L.G. Atencio et al., Nucl. Instr. and Meth. 187 (1981) 381.
[8] A.H. Walenta, Nucl. Instr. and Meth. 151 (1978) 461.
[9] A. Breskin, G. Charpak and F. Sauli, Nucl. Instr. and Meth. 151 (1978) 473.
[10] E-Division Semi-Annual Report, 1/79-6/79, p. 63; Los Alamos Report LA-8069-PR (1979) unpublished.
[11] F. Sauli, Nucl. Instr. and Meth. 156 (1978) 147.
[12] J.A. Edgington, Nucl. Instr. and Meth. 164 (1979) 175.
[13] M.W. McNaughton et al., Proc. 5th Int. Conf. on Polarization phenomena (Santa Fe, NM, 1980) (A.I.P. No. 69) p. 149.
[14] R.D. Ransome et al., ibid., p. 132.
[15] M.W. McNaughton, Internal report MP-13/MWM/X80-01 (1980).